THE JOURNAL OF PHYSICAL CHEMISTRY B

Article

pubs.acs.org/JPCB

Toward Understanding the Redox Properties of Model Chromophores from the Green Fluorescent Protein Family: An Interplay between Conjugation, Resonance Stabilization, and Solvent Effects

Debashree Ghosh, Atanu Acharya, Subodh C. Tiwari, and Anna I. Krylov*

Department of Chemistry, University of Southern California, Los Angeles, California 90089-0482, United States

Supporting Information

ABSTRACT: The redox properties of model chromophores from the green fluorescent protein family are characterized computationally using density functional theory with a long-range corrected functional, the equation-of-motion coupled-cluster method, and implicit solvation models. The analysis of electron-donating abilities of the chromophores reveals an intricate interplay between the size of the chromophore, conjugation, resonance stabilization, presence of heteroatoms, and solvent effects. Our best estimates of the gas-phase vertical/adiabatic detachment energies of the deprotonated (i.e., anionic) model red, green, and blue chromophores are 3.27/3.15, 2.79/2.67, and 2.75/2.35 eV, respectively. Vertical/adiabatic ionization energies of the respective protonated (i.e., neutral) species are 7.64/7.35, 7.38/7.15, and 7.70/7.32 eV, respectively. The standard reduction potentials (E^0_{red}) of the anionic ($Chr^{\bullet}/Chr^{-}$) and neutral ($Chr^{+\bullet}/Chr$) model chromophores in acetonitrile are 0.34/1.40 V (red), 0.22/1.24 V (green), and −0.12/1.02 V (blue), suggesting, counterintuitively, that the red chromophore is more difficult to oxidize than the green and blue ones (in both neutral and deprotonated forms). The respective redox potentials in water follow a similar trend but are more positive than the acetonitrile values.

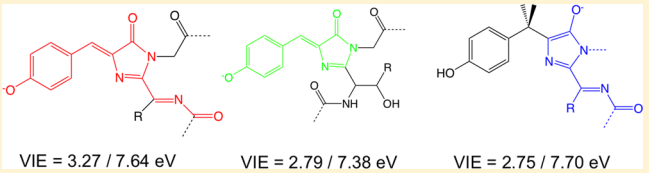

1. INTRODUCTION

Fluorescent proteins (FPs) from the green fluorescent protein (GFP) family are extensively used in bioimaging as genetically encoded fluorescent labels.[1−5] Motivated by a variety of exciting applications, a large number of FPs with different properties (color, Stokes shifts, brightness, photostability, phototoxicity, sensitivity to small ions, maturation rates, etc.) have been developed[6−9] covering the entire spectral range. Atomic-level understanding of their properties is important for engineering new designer FPs better suited for a particular application. This has been motivating extensive experimental and theoretical studies of their optical properties (excitation/emission energies and brightness), mechanistic details of chromophores' maturation, and the photocycle.[5,10−17]

Figure 1 shows selected chromophores of FPs of different color (the colors refer to fluorescence). The structural motifs of color tuning are rather diverse[17] and include chemical modifications of the chromophore such as extension of the π-system in the red FPs, π-stacking, and electrostatic interactions with the neighboring residues, as well as protonation−deprotonation equilibria. In stark contrast to their optical properties, relatively little is known about the redox properties and ionized/electron-detached states of these biomolecules.[18−20] The interest in these properties stems from the recent discovery that FPs can act as light-induced electron donors.[21] Redox-sensitive FPs can be used for *in vivo* measurements of the mitochondrial redox potential.[22,23] The focus of this work is on understanding the effect of structure of the chromophores on their redox properties. Better understanding of structure−function relationship can be used to develop novel fluorescent probes suited to new types of applications of genetically encoded FPs.

The properties of FPs are determined by the chemical structure of their chromophores and by the interactions of the chromophores with the surrounding protein. Following a bottom-up approach, we begin by investigating the redox properties of the model chromophores in the gas phase and in simple solvents. These calculations allow us to quantify the intrinsic electron-donating ability of the chromophores and to make inroads into understanding how the redox properties of the chromophores can be modulated by the environment (such as solvent and the nearby protein residues). Properties of model chromophores in the gas phase and simple solvents provide an important benchmark and can be measured experimentally.[24−26] Theoretical prediction of the low electron-detachment energy of the anionic form of the model GFP chromophore,[18,27] which suggested a metastable character of the bright excited state, has stimulated several experimental studies aiming at determining the detachment energy (DE) of this system.[28−30] With the exception of cyan FP,[29] the DEs of

Received: May 23, 2012
Revised: September 14, 2012
Published: September 14, 2012

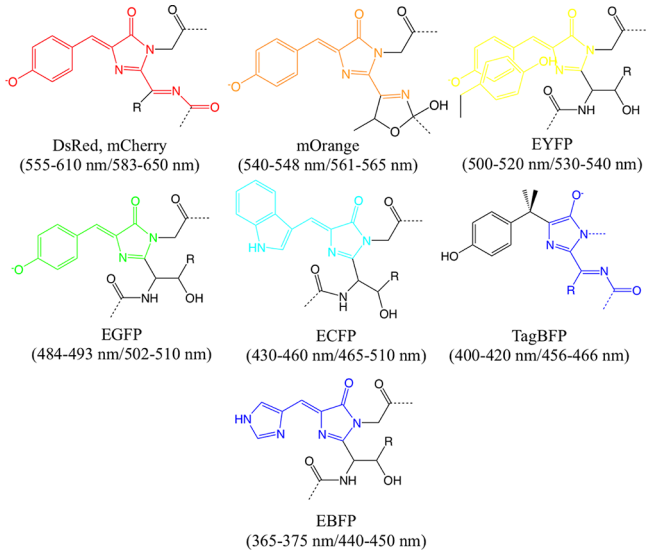

Figure 1. Chromophores of the selected FPs of different colors: wt-GFP, EGFP (green), TagBFP (blue), EBFP(blue), CFP (cyan), YFP (yellow), DsRed, mCherry (red), mOrange (orange). Absorption/emission wavelengths are given in parentheses. The chromophores are shown in colors corresponding to their fluorescence.

other isolated anionic chromophores have not yet been characterized. The first experimental measurement of the redox potential of neutral model GFP chromophores in solution has been recently reported.[20] This study demonstrated that the electron-donating ability of the chromophores can be modulated by varying resonance stabilization via structural modifications. The computational studies have helped to quantify solvent effects.[20,31] The redox potential of the protein-bound chromophore (EGFP) has only been characterized computationally.[19]

The electron donating ability of the chromophores depends on several delicately balanced factors, such as the size of the π-system, resonance stabilization of charge distributions, electronegativity of the atoms comprising the chromophore, and the presence of electron donating/withdrawing substituents, as well as solvent effects.

To illustrate these competing factors, consider homologically similar compounds of increasing size such as conjugated dyes or aromatic clusters. Using particle-in-the-box reasoning, one may anticipate that the energy levels (i.e., molecular orbitals) will be lowered in larger systems, resulting in red-shifted absorption and decrease in ionization energy (IE). In the same-size systems, energy can be lowered by resonance stabilization. Since the energetic consequences of delocalization are larger for charged systems, size increase and resonance stabilization have the opposite effect on electron ejection energies from neutral and anionic species. For example, the IEs of the neutral naphthalene clusters decrease with system size (8.14, 7.58, 7.56, and 7.49 eV for $(Nph)_n$, $n = 1-4$),[32] whereas the detachment energies (DEs) of the anionic naphthalene clusters increase with the system size (−0.18, 0.11, 0.28, 0.48, and 0.62 eV for $(Nph)_n^-$, $n = 1-5$).[33]

This trend is illustrated in Figure 2 for the electron-ejection processes from the neutral and anionic species:

$$HA \rightarrow HA^{+}(\text{radical - cation}) + e^{-}, \quad IE \tag{1}$$

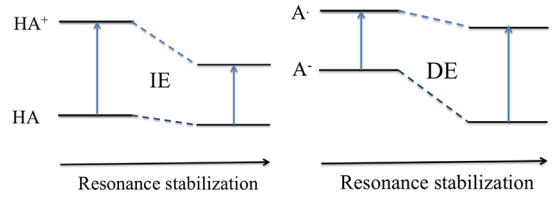

Figure 2. The effect of resonance stabilization on energetics of electron ejection from the neutral (left) and anionic (right) species. Since the resonance stabilization is greater for charged species, more extensive resonance interactions lead to ionization energy decrease in neutral species and to electron-detachment energy increase in anions.

$$A^{-}(\text{deprotonated}) \rightarrow A^{\bullet}(\text{neutral - radical}) + e^{-}, \quad DE \tag{2}$$

Here HA denotes neutral (protonated) species, such as neutral forms of the chromophores, whereas A^- denotes closed-shell anionic chromophores derived by the deprotonation of the respective neutral species. In the case of HA ionization, the HA^+ is strongly stabilized by resonance, leading to the IE decrease with increasing resonance stabilization, whereas, in the second reaction, the A^- is more stabilized by resonance than $A^{\bullet}$, leading to the DE increase.

Of course, the above considerations are valid only in homologically similar compounds. The IEs/DEs of isoelectronic species will be strongly modulated by the relative electronegativity of the constituent atoms and the presence of electron donating/withdrawing groups. For example, the effect of electronegativity of the heteroatoms can be illustrated by phenyl halides for which the IEs decrease when going from fluorine to iodine.[34] Finally, solvent will also affect energetics of the redox reactions, eqs 1 and 2. Polar solvent is expected to stabilize the charged species; more extensive resonance interactions leading to more delocalized charge are expected to reduce solvent stabilization. Thus, the effect of resonance stabilization on IEs/DEs will be offset by including solvent effects. In the previous study of the redox properties of model FP chromophores,[20] the trends in redox potentials were dominated by IEs of isolated chromophores; however, in the present study, we observe that solvent can even reverse the trends based on IEs.

In this work, we investigate the effect of the chromophore structure on the redox properties of model chromophores representing green (EGFP, wt-GFP), red (DsRed[35]), and blue (mTagBFP[36−38]) FPs (see Figure 1). Our aim is to quantify the competing factors described above laying out the foundation for developing qualitative models that can be used to rationalize and predict the trends in the redox properties based on the sizes of chromophores, resonance stabilization, and presence of heteroatoms. This is a prerequisite for future studies of the redox properties of the protein-bound chromophores.

This study focuses on the ground-state redox properties of FPs. The redox potentials of electronically excited chromophores, which are of interest in the context of light-induced electron-donating FPs,[21] can be estimated by using the following relationship between ground- and excited-state IEs:

$$IE^{ex} \approx IE^{gs} - E_{ex} \tag{3}$$

where IE^{ex} is the IE of the electronically excited chromophore, IE^{gs} is the IE of the ground state, and E_{ex} is the excitation energy. For example, the computed redox potential of EGFP is 0.55 V.[19] Using a computed vertical excitation energy of 2.70 eV, we arrive at $E^0 \approx -2.15$ V for electronically excited EGFP.

dx.doi.org/10.1021/jp305022t | J. Phys. Chem. B 2012, 116, 12398−12405

This is a lower-bound estimate, as it does not include relaxation of the chromophore and its protein environment in the electronically excited state.

Different protonation forms of the chromophores may exist in the protein and, especially, in solvents. For the model GFP chromophore, four different forms shown in Figure 3 have been considered,[39−41] i.e., neutral, anionic (deprotonated phenolic moiety), cationic (protonated imidazolinone), and zwitterionic. Since the neutral and anionic states appear to be most relevant to the FP photocycle,[1,4,5] we focus on these two forms of all model chromophores. We denote the deprotonated forms by "-D". Experiments carried out at different pH can give rise to chromophores in different protonation states.[42]

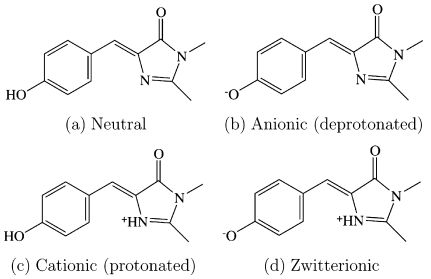

Figure 3. Different protonation states of the GFP model chromophore.

The model molecules representing the green, red, and blue chromophores are the following: (i) 4-hydroxybenzylidene-1,2-dimethylimidazolinone (HBDI), (ii) 4-hydroxybenzylidene-1-methyl-2-penta-1,4-dien-1-yl-imidazolin-5-one (HBMPDI), and (iii) *N*-[(5-hydroxy-1*H*-imidazole-2yl)methyl-methylidene]-acetamide (HIMA) and *N*-[(5-hydroxy-1*H*-imidazole-2yl) methylidene]acetamide (HHIMA), respectively. The structures of their deprotonated forms are shown in Figure.4

The structure of the paper is as follows. Section 2 gives computational details. Section 3 presents our results and discussion of the gas-phase energetics (section 3.1), solvent effects (section 3.2), and redox potentials (section 3.3) of the model compounds. Our concluding remarks are given in section 4.

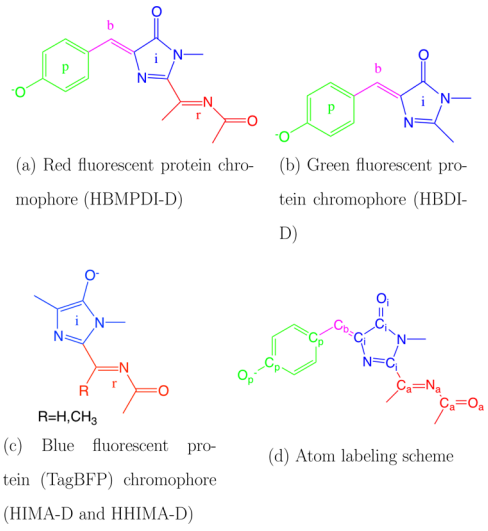

Figure 4. The structures of the model chromophores (deprotonated forms) and atom labeling scheme. The chromophores consist of the green (phenol), pink (bridge), blue (imidazolinone), and red (acylimine) moieties. Panel d gives the atom labeling scheme: "p", "b", "i", and "a" denote phenol, bridge, imidazolinone, and acylimine, respectively.

2. COMPUTATIONAL DETAILS

The structures of the model chromophores (see Figure 4) were optimized using RI-MP2/cc-pVTZ. Since MP2 is not reliable for open-shell species, the ionized species were optimized by density functional theory (DFT) with the ωB97X-D functional[43] and the cc-pVTZ basis set. The Cartesian geometries and relevant energies are given in the Supporting Information. The optimized structures were used for calculation of IEs and DEs with ωB97x-D. Two basis sets were employed: 6-311++G(2df,2pd) and 6-31+G(d). Zero point energy (ZPE) corrections to the adiabatic values as well as other thermodynamic corrections were computed by ωB97x-D/cc-pVTZ at the respective optimized geometries. In addition, IEs/DEs were calculated using the equation-of-motion coupled-cluster method with single and double substitutions for ionization potentials (EOM-IP-CCSD)[44−48] for comparison, in particular, to check for potential artifacts in the computed trends due to remaining self-interaction error. The EOM-IP-CCSD calculations were performed with the 6-31+G(d) basis set. On the basis of our recent calculations of phenol and phenolate,[49] we anticipate 0.1−0.3 eV differences between ωB97X-D and EOM-IP-CCSD. The estimated error bars for the IE/DE values computed with ωB97X-D are ≈0.1 eV.[50]

Natural bond orbital (NBO)[51] analysis of charge and spin densities was carried out to understand the structure−function correlations. The solvation free energies were computed using a continuum solvation model, SM8,[52] and the 6-31+G(d,p) basis set. The free energies of the redox reactions were calculated by constructing thermodynamic cycles as explained in section 3.3.

The main cause of error in the computed redox potentials is due to the calculation of solvation free energies with implicit solvation methods. A conservative estimate for the error bars of the solvation free energy is ≈0.4 eV based on the recent benchmark studies.[53,54] Explicit solvation methods with polarization effects can be used to calculate the free energy changes with higher accuracy. For example, the hybrid quantum mechanical/effective fragment potential (EFP) approach has shown errors of ∼0.05−0.1 eV with respect to high-level ab initio methods such as EOM-IP-CCSD.[55,49] However, these methods require extensive sampling which is computationally demanding for large chromophores.

All calculations were carried out using *Q-Chem*.[56]

3. RESULTS AND DISCUSSION

3.1. Ionization and Electron Detachment Energies of the Isolated Chromophores. Table 1 shows the vertical and adiabatic IEs/DEs (VIE/VDE and AIE/ADE, respectively) of the model blue (HIMA and HHIMA), green (HBDI), and red (HBMPDI) chromophores. For comparison, we also present energies for phenol and phenolate.[49] We have also tabulated the energies calculated using EOM-IP-CCSD. The IEs/DEs calculated by the EOM and DFT methods follow similar trends, which allows us to validate that the DFT results for the chromophores of different sizes are not affected by the remaining self-interaction error. We notice that the difference is relatively small for the neutral species (∼0.1 eV) and is about 0.3 eV for the anionic ones. Our previous study of phenol/

dx.doi.org/10.1021/jp305022t | J. Phys. Chem. B 2012, 116, 12398−12405

Table 1. Vertical and Adiabatic Ionization/Detachment Energies (eV) of the Model FP Chromophores and Phenolic Species[a]

species	Koopmans[b]	VIE/VDE	VIE/VDE (EOM-IP)[c]	AIE/ADE	AIE/ADE w/ ZPE	ΔG_g
HIMA	8.00	7.70	7.64	7.36	7.32	7.29
HHIMA	8.08	7.83	7.77	7.51	7.50	7.48
HBDI	7.59	7.38	7.33	7.15	7.15	7.13
HBMPDI	7.94	7.64	7.59	7.35	7.35	7.31
phenol		8.55	8.55[d]			
HIMA-D	2.97	2.75	2.43	2.33	2.35	2.35
HHIMA-D	3.07	2.90	2.58	2.61	2.63	2.59
HBDI-D	2.94	2.79	2.48	2.67	2.67	2.66
HBMPDI-D	3.45	3.27	3.01	3.15	3.15	3.11
Phenolate		2.22	1.99[d]			

[a] ωB97x-D/6-311++G(2df,2pd). [b] Hartree–Fock HOMO energy, 6-311++G(2df,2pd). [c] EOM-IP-CCSD/6-31+G(d). [d] From ref 49, EOM-IP-CCSD/cc-pVTZ.

phenolate[49] suggests that EOM-IP-CCSD/cc-pVTZ underestimates the DEs of anionic species, e.g., the errors for VDE of phenolate were 0.3 eV. We note that the ωB97X-D/6-311(+,+)G(2pd,2df) value for phenolate (see Table 1) is in much better agreement with the experimental VDE of 2.36 eV.[57,58] Recent experiments[29,30] have reported a 2.8 eV VDE for gas-phase HBDI-D, which is close to the computed ωB97X-D/6-311(+,+)G(2pd,2df) value (Table 1) but is about 0.3 eV higher than the EOM-IP value from Table 1 and, consequently, the previously reported theoretical estimate[27,18] derived using the EOM-IP based energy additivity scheme. Thus, in this work, we rely on ωB97X-D/6-311(+,+)G(2pd,2df) for DE/IE calculations. The EOM-IP values are used to validate that the differences between the chromophores of different sizes are not affected by remaining self-interaction error.

Our best estimates (in eV) for VIE/VDEs are 7.38/2.79 (HBDI), 7.64/3.27 (HBMPDI), 7.83/2.90 (HHIMA), and 7.70/2.75 (HIMA) for the neutral/deprotonated forms. The best estimates of the respective adiabatic values (AIE/ADEs) are 7.15/2.67 (HBDI), 7.35/3.15 (HBMPDI), 7.50/2.63 (HHIMA), and 7.32/2.35 (HIMA) for the protonated and deprotonated forms.

As discussed above, we expect that resonance stabilization will have the opposite effect in the neutral and anionic (deprotonated) species. The leading resonance structures of the anionic chromophores are shown in Figure 5. As one can see, the red chromophore has the most extensive resonance stabilization. The comparison between HIMA and HBDI is more complicated due to only partial overlap of their structural frameworks.

Let us first consider trends in the anionic species. Among the deprotonated species, phenolate has the lowest DE (1.99 eV). The VDE of HBMPDI-D, which is the largest system, is the highest (3.27 eV) due to more extensive resonance stabilization than in the HIMA-D and HBDI-D anions. The VDEs of HIMA-D and HBDI-D are 2.75 and 2.79 eV, respectively. HIMA-D (methylated species) has a lower DE than HHIMA-D (nonmethylated) due to the electron-donating methyl group. Interestingly, despite sizable differences in VDEs of phenolate, HBDI-D, and HBMPDI-D, the analysis of spin densities reveals that electron detachment occurs predominantly from the phenolate moiety (see Table 3 in section 3.1.1). In order to further support our theory, we calculated the VIEs of the ortho, meta, and para isomers of deprotonated HBDI. We see the opposite trend from its protonated counterparts,[20] as expected.

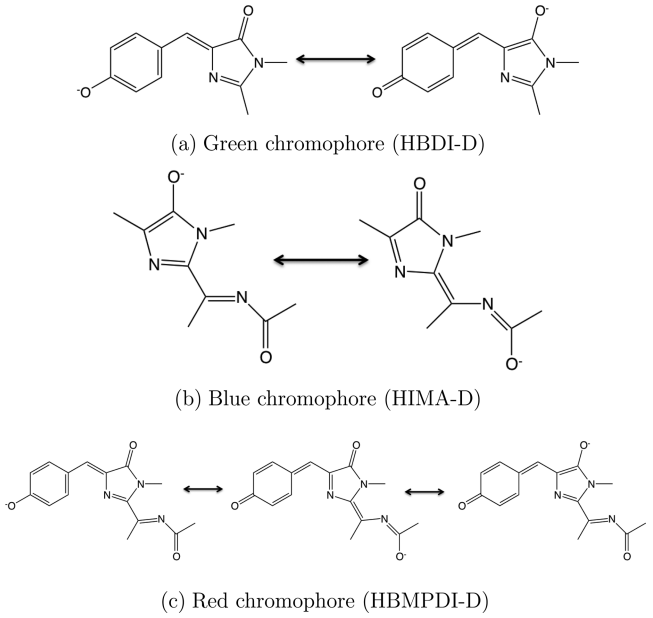

Figure 5. Leading resonance structures of the deprotonated model FP chromophores. Other resonance structures are given in the Supporting Information.

Among the neutral species, phenol has the highest IE (1 eV higher than that of HBDI), as expected. The difference between HIMA and HHIMA is again due to the electron-donating methyl group. However, we note that HBDI has a lower IE than HBMPDI, contrary to the trend in Figure 2. This can be rationalized by close inspection of the structural parameters summarized in Table 2, revealing that the difference in resonance stabilization in HBDI and HBMPDI is larger in the anionic forms (relative to $HBDI^+$ and $HBMPDI^+$). In the case of ionized (cationic) HBDI and HBMPDI, the degree of resonance stabilization involving the phenol, bridge, and imidazolinone moieties appears to be very similar, judging by the similarity of the C_p-C_b and C_i-C_b bond lengths in $HBDI^+$ and $HBMPDI^+$ (see Table 2). This is further supported by the charges on O_p and O_i (−0.58 and −0.47 in $HBDI^+$ and $HBMPDI^+$). The IE values of HBDI and HBMPDI are determined by the two competing effects, more extended resonance stabilization due to acylimine and electron-withdrawing character of this moiety (which contains several electro-negative atoms), and based on the computed IE values, the latter appears to be more important in this case.

3.1.1. Quantifying Resonance Interaction by Structural Analysis. The degree of resonance interactions in these species can be quantified by the representative geometric parameters collected in Table 2 (see Figure 4 for the atom labeling scheme).

Comparing the C_p-C_b and C_i-C_b bond lengths in reduced/oxidized HBDI and HBMPDI, we see that the bond length alternation is lower in the case of the ionized form of the neutral (HA^+) and the anionic form of the deprotonated (A^-) species, as expected.

We define $\Delta = \sqrt{(\sum_{i=1}^{n} (r_i - \bar{r})^2)}$, where $\bar{r}$ is the average bond length of a given type (e.g., C–N bond in imidazolinone), which quantifies the degree of bond length alternation and,

dx.doi.org/10.1021/jp305022t | J. Phys. Chem. B 2012, 116, 12398–12405

Table 2. Selected Geometric Parameters (Å) of the Model Chromophores and the Respective Oxidized Species[a]

species	C_p-C_b	C_i-C_b	O_p-C_p	O_i-C_i	$\sigma(C_s-N_s)$	$\Delta(N_i-C_i)$	$\Delta(C_p-C_p)$
HIMA	n.a.	1.490	n.a.	1.353	0.127	0.014	n.a.
HIMA(ionized)	n.a.	1.476	n.a.	1.297	0.171	0.029	n.a.
HIMA-D	n.a.	1.487	n.a.	1.245	0.045	0.021	n.a.
HIMA-D(ionized)	n.a.	1.477	n.a.	1.211	0.145	0.026	n.a.
HBDI	1.435	1.349	1.354	1.209	n.a.	0.049	0.008
HBDI(ionized)	1.397	1.390	1.319	1.197	n.a.	0.004	0.028
HBDI-D	1.393	1.385	1.248	1.236	n.a.	0.050	0.040
HBDI-D(ionized)	1.413	1.369	1.228	1.209	n.a.	0.038	0.046
HBMPDI	1.447	1.345	1.351	1.208	0.132	0.045	0.009
HBMPDI(ionized)	1.395	1.393	1.316	1.197	0.153	0.004	0.029
HBMPDI-D	1.385	1.394	1.234	1.226	0.093	0.033	0.045
HBMPDI-D(ionized)	1.404	1.377	1.226	1.208	0.134	0.028	0.048

[a] $\sigma(C_s-N_s)$ and Δ quantify the degree of bond length alternation in acylimine and phenolate/imidazolinone moieties, respectively (see text). The atom labeling scheme is given in Figure 4d.

therefore, resonance stabilization. Likewise, $\sigma(C_s-N_s)$ is defined as the difference between the two C_s-N bonds in acylimine. Comparing Δ's computed for the phenolate and imidazolinone rings shows that $HBMPDI^+$ exhibits a similar degree of resonance stabilization as $HBDI^+$. HBMPDI-D has a lower Δ(imidazolinone) than HBDI-D, while the respective Δ(phenolate) values are similar. This is because the imidazolinone in HBMPDI-D is further stabilized due to the additional resonance structure (see Figure 5).

We further analyze the degree of delocalization and resonance stabilization by comparing the relevant NBO charges and spin densities. The molecules can be divided into different parts, as shown in Figure 4 and Supporting Information. Table 3 shows the spin densities ($\rho_\alpha-\rho_\beta$) on the different moieties of the oxidized chromophores quantifying the location of the unpaired electron.

Table 3. Mulliken Analysis of Spin Densities in the Oxidized Species

species	phenol	imidazolinone	bridge	acylimine
HBDI	0.41	0.59	0.00	n.a.
HBMPDI	0.39	0.60	−0.02	0.03
HHIMA	n.a.	0.86	0.02	0.12
HBDI-D	0.73	0.51	−0.24	n.a.
HBMPDI-D	0.68	0.52	−0.25	0.05
HHIMA-D	n.a.	0.80	0.00	0.19

In the case of both forms of HBDI and HBMPDI, we observe that the ionization involves both the phenol and imidazolinone moieties, with phenol/phenolate playing the leading role in deprotonated species (the imidazolinone hosts a larger fraction of the spin density in $HBDI^+$ and $HBMPDI^+$). The spin densities on acylimine are smaller in the case of HBMPDI/HBMPDI-D than in HHIMA/HHIMA-D. Therefore, acylimine plays a less important role in the red chromophore than in the blue one.

The highest occupied molecular orbitals (HOMOs) are shown in Figure 6. Comparing the HOMOs for HBMPDI and HBMPDI-D, we note that there is less electron density on the C_i-C_s bond and acylimine in the case of the protonated species. The HOMO of HBMPDI is similar to that of HBDI—it is delocalized over phenol and imidazolinone but does not have much density on acylimine. However, the HOMO of HBDI-D is somewhat different from that of HBMPDI-D, showing a different degree of delocalization.

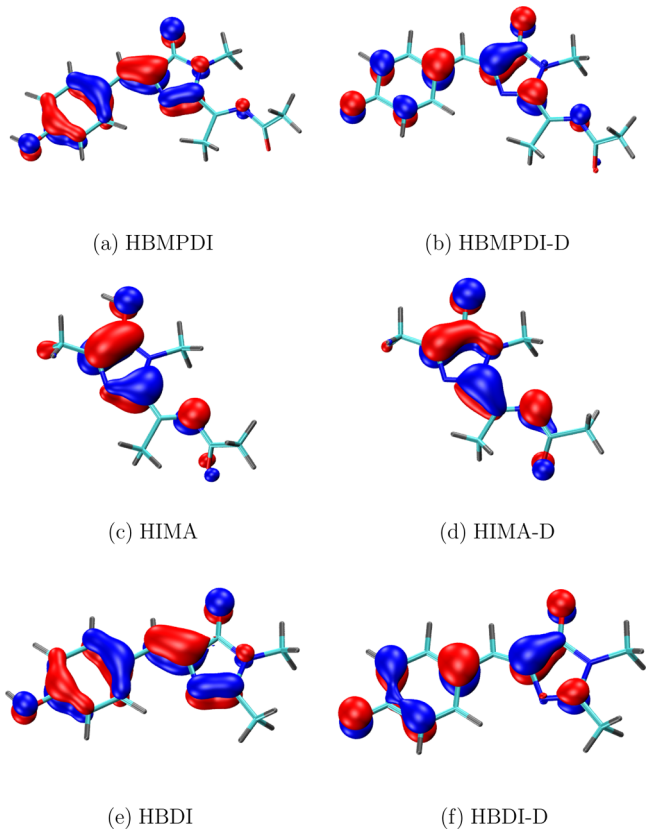

Figure 6. The HOMOs of the model chromophores.

3.2. Solvent Effects. Table 4 shows solvation free energies for the relevant species as well as $\Delta\Delta G_{solv}$ in acetonitrile, the solvent contribution to the free energy of the oxidation reactions, eqs 1 and 2. For most of the species, the $\Delta\Delta G_{solv}$'s in acetonitrile follow an opposite trend relative to IE/DEs. This is because the solvent stabilization is larger for more localized charges. Thus, the greater the stability of the charged species (due to charge delocalization), the lower is its solvation free energy. For example, charge distribution shows that HBMPDI-D has the most charge delocalization and $HHIMA^+$ has the least charge delocalization (among the charged species). They

dx.doi.org/10.1021/jp305022t | J. Phys. Chem. B 2012, 116, 12398−12405

Table 4. Free Energies of Solvation (kcal mol^{-1}) in Acetonitrile for the Model Chromophores

species	ΔG_{red}	ΔG_{ox}	$\Delta\Delta G_{solv}$
HIMA	−11.85	−57.65	−45.80
HHIMA	−12.05	−58.01	−45.96
HBDI	−15.33	−52.52	−37.19
HBMPDI	−16.95	−54.63	−37.68
HIMA-D	−52.52	−10.78	+41.74
HHIMA-D	−53.12	−9.91	+43.21
HBDI-D	−57.87	−15.56	+42.31
HBMPDI-D	−51.63	−16.79	+34.84

have the lowest and highest ΔG_{solv}, respectively, the trend which is carried over to the $\Delta\Delta G_{solv}$'s.

We observe similar trends for solvation energies in water (Table 5). We also note that the difference between $\Delta\Delta G_{solv}$ is

Table 5. Free Energies of Solvation (kcal mol^{-1}) in Water for the Model Chromophores

species	ΔG_{red}	ΔG_{ox}	$\Delta\Delta G_{solv}$
HIMA	−10.96	−56.82	−45.86
HHIMA	−12.22	−58.06	−45.84
HBDI	−12.06	−47.65	−35.59
HBMPDI	−13.24	−49.50	−36.26
HIMA-D	−56.03	−8.07	+47.96
HHIMA-D	−57.82	−7.95	+49.87
HBDI-D	−60.01	−11.22	+48.79
HBMPDI-D	−52.68	−11.80	+40.88

very similar for acetonitrile and water in the case of neutral species (~0.77 kcal mol^{-1} difference on average) but is somewhat shifted for the deprotonated species (~6.35 kcal mol^{-1} difference on average).

3.3. Redox Potentials. From the energetics of ionization/electron-detachment and solvation processes, we can construct a thermodynamic cycle (Figure 7) using Hess' law:

$$\Delta G_{rxn} = \Delta G_g + (\Delta G_{ox} - \Delta G_{red})$$

$$E^0_{ox} = -\frac{\Delta G_{rxn}}{nF} \quad (4)$$

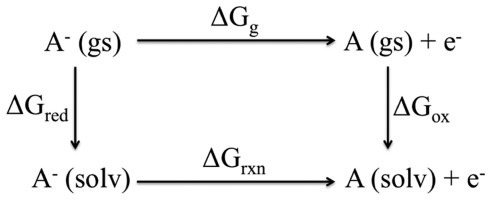

Figure 7. Thermodynamic cycle.

where n is the number of electrons involved in the redox reaction and F is Faraday's constant. We note that gas-phase Gibbs free energy changes of the oxidation reactions, ΔG_g, are very close to ADEs (the differences do not exceed 0.04 eV, see Table 1 and the Supporting Information). Using this equation, we calculated E^0_{ox} with respect to the standard hydrogen electrode (SHE). Here, we have taken the ΔG of SHE to be the recent value of −4.281 V.[59] The reported values can easily be converted to the potentials relative to more commonly used reference electrodes, e.g., a ferrocene couple (Fc^+/Fc) used in ref 20. The calculated redox potentials of the FP model chromophores in acetonitrile and water are given in Table 6.

Table 6. Standard Reduction Potentials versus SHE (E^0, V) in Acetonitrile and Water for the Model Protein Chromophores (HA^+/HA and $A^\bullet$/A^-)

species	E^0(acetonitrile)	E^0(water)
HIMA	1.02	1.03
HHIMA	1.21	1.21
HBDI	1.24	1.31
HBMPDI	1.40	1.46
HIMA-D	−0.12	0.15
HHIMA-D	0.18	0.47
HBDI-D	0.22	0.50
HBMPDI-D	0.34	0.60

Experimentally, anionic chromophores can only be prepared in water (at high pH); thus, the computed E^0 in acetonitrile cannot be verified experimentally. However, these values are useful for theoretical analysis, as they allow us to compare neutral versus anionic chromophores in the same nonprotic solvent, and to quantify the effect of solvent polarity on different species. On the basis of the previous study,[20] the errors in absolute values of the E^0s computed using this protocol were around 0.2 V; however, the differences between different chromophores were reproduced by theory more accurately (maximum error of 0.08 V). Thus, the differences in computed E^0 for different chromophores are larger than the anticipated error bars of the method employed.

The trends in redox potentials of the chromophores are dominated by IEs/DEs. However, since solvent stabilization ($\Delta\Delta G_{solv}$) follows an opposite trend from the IEs/DEs, it offsets the differences in IEs/DEs and can even reverse the overall energetics when the differences in IEs/DEs are small. Consequently, the variations in the redox potentials are smaller relative to the differences in the respective IEs/DEs. This also follows from the empirical equations for the calculation of redox potentials from VIEs.[60]

We note that the redox potentials of aqueous HBDI and HBMPDI are close to E^0 of phenol (1.32 V);[49] however, the potentials for the respective anionic species are somewhat lower than that of phenolate (0.89 V, ref 49).

In our previous work on the ortho, meta, and para isomers of HBDI,[20] we observed that the trend in redox potentials is dominated by the variations of IEs, since solvent effects for structurally similar chromophores are similar. In the present study, however, the chromophores are significantly different and have different solvation free energies. Because of these two opposing effects, the trends in the redox potentials sometimes differ from the IE/DE predictions, e.g., the redox potential of the neutral blue chromophore is lower than that of the red and green chromophores, although the IEs of the red and green chromophores are lower than those of the blue one. Therefore, both the IEs/DEs as well as effects of solvation are important for understanding the trends in the redox potentials. Moreover, the observed solvent effects suggest that protein environment can strongly modulate the redox properties of the protein-bound chromophores by electrostatic interactions. For example, one can anticipate different redox potentials for families of FPs sharing the same chromophore but having different local environment. These effects will be investigated in future studies. As of today, the only available estimate of E^0 of a

dx.doi.org/10.1021/jp305022t | J. Phys. Chem. B 2012, 116, 12398−12405

protein-bound chromophore is for EGFP.[19] The value reported in ref 19 (0.47 V) was computed using $\Delta G = -4.36$ V for SHE. Thus, for the corrected value using a more recent value of SHE (−4.281 V), we arrive at 0.55 V. The computational protocol used in ref 19 was rather crude, suggesting error bars of about 0.1−0.2 V. Within these error bars, the computed E^0 of the protein-bound anionic green chromophore is indistinguishable from E^0 of HBDI-D in aqueous solution. Thus, although protein as a whole is less polar than water, the nearby charged groups (such as argenine) provide a strong stabilizing effect for the anionic chromophore, making its electron-donating ability comparable to that of the isolated chromophore in aqueous solution. The comparison of the acetonitrile value and E^0 of the protein-bound chromophore shows that the protein environment provides stronger stabilizing effects as compared to acetonitrile. On the basis of these comparisons, one can use the E^0 values of a chromophore in water and acetonitrile as very crude estimates bracketing the redox potential of the protein-bound chromophore. However, more data on the redox properties of FPs and their bare chromophores are necessary to understand the range of the effect of protein environment on E^0.

4. CONCLUSIONS

We performed a detailed computational study of the electron-donating abilities of the three model chromophores representing green, red, and blue FPs. The calculations reveal that the energetics of ionization/electron detachment processes depends on a delicate balance between resonance stabilization and electronegativity considerations. The main trends in IEs/DEs can be explained by the charge stabilization due to extended resonance. Since the effect of resonance stabilization is more important in charged species, the respective energetics follows opposite trends in the neutral and anionic chromophores. However, this trend can be offset by electronegativity of atoms constituting the chromophores. Somewhat counterintuitively, the red chromophore has a higher DE/IE than the green chromophore.

The solvation free energies follow the opposite trends than IEs/DEs. The redox potentials are predominantly driven by IEs/DEs; however, the difference in redox potentials between the species is much smaller than gas-phase energetics would imply. Moreover, solvent effects can even reverse the trend based on IEs/DEs. Thus, protein environment is expected to have a significant effect on the redox properties of the chromophores.

■ ASSOCIATED CONTENT

Supporting Information

Additional information about the ionization energies calculated at different levels of theory, detailed calculation of free energies from thermodynamic data, resonance structures and geometries of the chromophores. This material is available free of charge via the Internet at http://pubs.acs.org.

■ AUTHOR INFORMATION

Notes

The authors declare no competing financial interest.

■ ACKNOWLEDGMENTS

A.I.K. acknowledges support from the National Science Foundation through the CHE-0951634 grant and from the Humboldt Research Foundation (Bessel Award). A.I.K. is deeply indebted to the Dornsife College of Letters, Arts, and Sciences and the WISE program (USC) for bridge funding support.

■ REFERENCES

(1) Heim, R.; Prasher, D. C.; Tsien, R. Y. *Proc. Natl. Acad. Sci. U.S.A.* **1994**, *91*, 12501.
(2) Tsien, R. Y. *Annu. Rev. Biochem.* **1998**, *67*, 509.
(3) Day, R. N.; Davidson, M. W. *Chem. Soc. Rev.* **2009**, *38*, 2887.
(4) Zimmer, M. *Chem. Rev.* **2002**, *102*, 759.
(5) Meech, S. R. *Chem. Soc. Rev.* **2009**, *38*, 2922.
(6) Zhang, J.; Campbell, R. E.; Ting, A. Y.; Tsien, R. Y. *Nature* **2002**, *3*, 906.
(7) Giepmans, B. N. G.; Adams, S. R.; Ellisman, M. H.; Tsien, R. Y. *Science* **2006**, *312*, 217.
(8) Nguyen, A. W.; Daugherty, P. S. *Nat. Biotechnol.* **2005**, *23*, 355.
(9) Shaner, N. C.; Steinbach, P. A.; Tsien, R. Y. *Nat. Methods* **2005**, *2*, 905.
(10) Lukyanov, K. A.; Serebrovskaya, E. O.; Lukyanov, S.; Chudakov, D. M. *Photochem. Photobiol. Sci.* **2010**, *9*, 1301.
(11) Lovell, J. F.; Liu, T. W. B.; Chen, J.; Zheng, G. *Chem. Rev.* **2010**, *110*, 2839.
(12) Wachter, R. M. *Photochem. Photobiol.* **2006**, *82*, 339.
(13) Yan, W.; Zhang, L.; Xie, D.; Zheng, J. *J. Phys. Chem. B* **2007**, *111*, 14055.
(14) van Thor, J. J. *Chem. Soc. Rev.* **2009**, *38*, 2935.
(15) Tolbert, L. M.; Baldridge, A.; Kowalik, J.; Solntsev, K. M. *Acc. Chem. Res.* **2012**, *45*, 171.
(16) Nemukhin, A. V.; Grigorenko, B. L.; Savitskii, A. P. *Acta Nat.* **2009**, *2*, 41.
(17) Bravaya, K. B.; Grigorenko, B. L.; Nemukhin, A. V.; Krylov, A. I. *Acc. Chem. Res.* **2012**, *45*, 265.
(18) Epifanovsky, E.; Polyakov, I.; Grigorenko, B. L.; Nemukhin, A. V.; Krylov, A. I. *J. Chem. Phys.* **2010**, *132*, 115104.
(19) Bravaya, K. B.; Khrenova, M. G.; Grigorenko, B. L.; Nemukhin, A. V.; Krylov, A. I. *J. Phys. Chem. B* **2011**, *8*, 8296.
(20) Solntsev, K. M.; Ghosh, D.; Amador, A.; Josowicz, M.; Krylov, A. I. *J. Phys. Chem. Lett.* **2011**, *2*, 2593.
(21) Bogdanov, A. M.; Mishin, A. S.; Yampolsky, I. V.; Belousov, V. V.; Chudakov, D. M.; Subach, F. V.; Verkhusha, V. V.; Lukyanov, S.; Lukyanov, K. A. *Nat. Chem. Biol.* **2009**, *5*, 459.
(22) Dooley, C. T.; Dore, T. M.; Hanson, G. T.; Jakson, W. C.; Remington, S. G.; Tsien, R. Y. *J. Biol. Chem.* **2004**, *279*, 2284.
(23) Hanson, G. T.; Aggeler, R.; Oglesbee, D.; Cannon, M.; Capaldi, R. A.; Tsien, R. Y.; Remington, S. J. *J. Biol. Chem.* **2004**, *279*, 13044.
(24) Nielsen, S. B.; Lapierre, A.; Andersen, J. U.; Pedersen, U. V.; Tomita, S.; Andersen, L. H. *Phys. Rev. Lett.* **2001**, *87*, 228102.
(25) Andersen, L. H.; Lappierre, A.; Nielsen, S. B.; Nielsen, I. B.; Pedersen, S. U.; Pedersen, U. V.; Tomita, S. *Eur. Phys. J. D* **2002**, *20*, 597.
(26) Dong, J.; Solntsev, K. M.; Tolbert, L. M. *J. Am. Chem. Soc.* **2006**, *128*, 12038.
(27) Epifanovsky, E.; Polyakov, I.; Grigorenko, B. L.; Nemukhin, A. V.; Krylov, A. I. *J. Chem. Theory Comput.* **2009**, *5*, 1895.
(28) Forbes, M. W.; Jockusch, R. A. *J. Am. Chem. Soc.* **2009**, *131*, 17038.
(29) Mooney, C. R. S.; Sanz, M. E.; McKay, A. R.; Fitzmaurice, R. J.; Aliev, A. E.; Caddick, S.; Fielding, H. H. *J. Phys. Chem. A* **2012**, *116*, 7943−7949.
(30) Horke, D. A.; Verlet, J. R. R. *Phys. Chem. Chem. Phys.* **2012**, *14*, 8511.
(31) Zuev, D.; Bravaya, K.; Makarova, M. V.; Krylov, A. I. *J. Chem. Phys.* **2011**, *135*, 194304.
(32) Fujiwara, T.; Lim, E. C. *J. Phys. Chem. A* **2003**, *107*, 4381.
(33) Song, J. K.; Han, S. Y.; Kim, J. H.; Kim, S. K.; Lyapustina, S. A.; Xu, S.; Niles, J. M.; Bowen, K. H. *J. Chem. Phys.* **2002**, *116*, 4477.

(34) Baker, A. D.; Betteridge, D.; Kemp, N. R.; Kirby, R. E. *Int. J. Mass Spectrom. Ion Phys.* **1970**, *4*, 90.
(35) Shcherbo, D.; Merzlyak, E. M.; Chepurnykh, T. V.; Fradkov, A. F.; Ermakova, G. V.; Solovieva, E. A.; Lukyanov, K. A.; Bogdanova, E. A.; Zaraisky, A. G.; Lukyanov, S.; Chudakov, D. M. *Nat. Methods* **2007**, *4*, 741.
(36) Subach, O. S.; Malashkevich, V. N.; Zencheck, W. D.; Morozova, K. S.; Piatkevich, K. D.; Almo, S. C.; Verkhusha, V. V. *Chem. Biol.* **2010**, *17*, 333.
(37) Subach, O. M.; Cranfill, P. J.; Davidson, M. W.; Verkhusha, V. V. *PLoS One* **2011**, *6*, e28674.
(38) Bravaya, K. B.; Subach, O.; Korovina, N.; Verkhusha, V. V.; Krylov, A. I. *J. Am. Chem. Soc.* **2012**, *134*, 2807.
(39) Voityuk, A. A.; Michel-Beyerle, M.-E.; Rösch, N. *Chem. Phys. Lett.* **1997**, *272*, 162.
(40) Das, A. K.; Hasegawa, J.-Y.; Miyahara, T.; Ehara, M.; Nakatsuji, H. *J. Comput. Chem.* **2003**, *24*, 1421.
(41) Polyakov, I.; Grigorenko, B. L.; Epifanovsky, E.; Krylov, A. I.; Nemukhin, A. V. *J. Chem. Theory Comput.* **2010**, *6*, 2377.
(42) Bizzari, R.; Archangeli, C.; Arosio, D.; Ricci, F.; Faraci, P.; Cardarelli, F.; Beltram, F. *Biophys. J.* **2006**, *90*, 3300.
(43) Chai, J.-D.; Head-Gordon, M. *Phys. Chem. Chem. Phys.* **2008**, *10*, 6615.
(44) Sinha, D.; Mukhopadhyay, D.; Mukherjee, D. *Chem. Phys. Lett.* **1986**, *129*, 369.
(45) Stanton, J. F.; Gauss, J. *J. Chem. Phys.* **1994**, *101*, 8938.
(46) Pieniazek, P. A.; Arnstein, S. A.; Bradforth, S. E.; Krylov, A. I.; Sherrill, C. D. *J. Chem. Phys.* **2007**, *127*, 164110.
(47) Pieniazek, P. A.; Bradforth, S. E.; Krylov, A. I. *J. Chem. Phys.* **2008**, *129*, 074104.
(48) Krylov, A. I. *Annu. Rev. Phys. Chem.* **2008**, *59*, 433.
(49) Ghosh, D.; Roy, A.; Seidel, R.; Winter, B.; Bradforth, S.; Krylov, A. I. *J. Phys. Chem. B* **2012**, *116*, 72697280.
(50) Chai, J.-D.; Head-Gordon, M. *J. Chem. Phys.* **2008**, *128*, 084106.
(51) Weinhold, F.; Landis, C. R. *Chem. Educ.: Res. Pract. Eur.* **2001**, *2*, 91.
(52) Cramer, C. J.; Truhlar, D. G. *Acc. Chem. Res.* **2008**, *41*, 760.
(53) Marenich, A. V.; Cramer, C. J.; Truhlar, D. G. *J. Phys. Chem. B* **2009**, *113*, 6378.
(54) Sviatenko, L.; Isayev, O.; Gorb, L.; Hill, F. C.; Lezczynski, J. *J. Comput. Chem.* **2011**, *32*, 2195.
(55) Ghosh, D.; Isayev, O.; Slipchenko, L. V.; Krylov, A. I. *J. Phys. Chem. A* **2011**, *115*, 6028.
(56) Shao, Y.; Fusti-Molnar, L.; Jung, Y.; Kussmann, J.; Ochsenfeld, C.; Brown, S.; Gilbert, A. T. B.; Slipchenko, L. V.; Levchenko, S. V.; O'Neill, D. P.; Distasio, R. A., Jr.; Lochan, R. C.; Wang, T.; Beran, G. J. O.; Besley, N. A.; Herbert, J. M.; Lin, C. Y.; Van Voorhis, T.; Chien, S. H.; Sodt, A.; Steele, R. P.; Rassolov, V. A.; Maslen, P.; Korambath, P. P.; Adamson, R. D.; Austin, B.; Baker, J.; Bird, E. F. C.; Daschel, H.; Doerksen, R. J.; Dreuw, A.; Dunietz, B. D.; Dutoi, A. D.; Furlani, T. R.; Gwaltney, S. R.; Heyden, A.; Hirata, S.; Hsu, C.-P.; Kedziora, G. S.; Khalliulin, R. Z.; Klunziger, P.; Lee, A. M.; Liang, W. Z.; Lotan, I.; Nair, N.; Peters, B.; Proynov, E. I.; Pieniazek, P. A.; Rhee, Y. M.; Ritchie, J.; Rosta, E.; Sherrill, C. D.; Simmonett, A. C.; Subotnik, J. E.; Woodcock, H. L., III; Zhang, W.; Bell, A. T.; Chakraborty, A. K.; Chipman, D. M.; Keil, F. J.; Warshel, A.; Hehre, W. J.; Schaefer, H. F., III; Kong, J.; Krylov, A. I.; Gill, P. M. W.; Head-Gordon, M. *Phys. Chem. Chem. Phys.* **2006**, *8*, 3172.
(57) Eland, J. H. D. *Int. J. Mass Spectrosc. Ion Phys.* **1969**, *2*, 471.
(58) Richardson, J. H.; Stephenson, L. M.; Brauman, J. I. *J. Am. Chem. Soc.* **1975**, *97*, 2967.
(59) Isse, A. A.; Gennaro, A. *J. Phys. Chem. B* **2010**, *114*, 7894.
(60) Crespo-Hernández, C. E.; Close, D. M.; Gorb, L.; Leszczynski, J. *J. Phys. Chem. B* **2007**, *111*, 5386.